

# A high-efficiency Transition Radiation Detector for high-counting-rate environments

M. Petrovici<sup>a,\*</sup>, M. Petriș<sup>a</sup>, I. Berceanu<sup>a</sup>, V. Simion<sup>a</sup>, D. Bartoș<sup>a</sup>, V. Cătănescu<sup>a</sup>,  
A. Herghelegiu<sup>a</sup>, C. Măgureanu<sup>a</sup>, D. Moisă<sup>a</sup>, A. Radu<sup>a</sup>, M. Klein-Bösing<sup>b</sup>, J.P. Wessels<sup>b</sup>,  
A. Wilk<sup>b</sup>, A. Andronic<sup>c</sup>, C. Garabatos<sup>c</sup>, R. Simon<sup>c</sup>, F. Uhlig<sup>c</sup>

<sup>a</sup>National Institute for Nuclear Physics and Engineering, Bucharest, Romania

<sup>b</sup>University of Münster, Germany

<sup>c</sup>Gesellschaft für Schwerionenforschung, Darmstadt, Germany

Received 21 May 2007; accepted 6 June 2007

Available online 16 June 2007

## Abstract

A prototype Transition Radiation Detector (TRD) with a new configuration was built and tested. The prototype consists of two individual multiwire proportional chambers (MWPC) that share a thin common central pad readout electrode. Measurements with a <sup>55</sup>Fe source and e, π and p of 1.5 GeV/c showed a very good energy, position resolution and a better e/π discrimination compared to the standard structure with a single MWPC. No significant deterioration of the resolutions is observed up to counting rates of  $2 \times 10^5$  particles cm<sup>-2</sup> s<sup>-1</sup>. These results open the possibility of constructing TRDs with a high e/π discrimination and granularity even for high-counting rate experiments with a reasonable number of layers.

© 2007 Elsevier B.V. All rights reserved.

PACS: 29.40.Cs

Keywords: Gaseous detectors; High-counting rate; High efficiency; e/π discrimination; Transition radiation detectors

## 1. Introduction

Transition Radiation Detectors (TRD) are proposed for lepton identification with the CBM experiment [1] at the future FAIR [2] facility at GSI. Currently, two large area TRD detectors are under construction for LHC experiments. One of them, the Transition Radiation Tracker (TRT) of the ATLAS experiment is based on straw tubes and fulfills the requirement of conserving its performance up to  $20 \times 10^6$  particles s<sup>-1</sup> per straw [3] at moderate occupancies per event in p–p collisions [4]. The second one, the ALICE-TRD is based on multiwire chambers and has a high-granularity readout electrode in order to maintain its performance up to the highest multiplicity anticipated in Pb + Pb collisions at LHC [5]. In contrast, CBM will be a fixed target heavy-ion experiment in the

energy range of 5–35 A GeV. Aimed to look for rare probes using the unique performance of FAIR in terms of high-intensity heavy-ion beam, it requires the combined performance of the two types of detectors mentioned before, i.e. a high-granularity and a good performance in a high-counting rate environment.

Simple Multiwire Proportional Chambers (MWPC) are obvious candidates for high-granularity fast detectors if the thickness of gas volume is reduced such to reach the required counting rate performance. Up to intensities of  $10^5$  particles cm<sup>-2</sup> s<sup>-1</sup> no major deterioration of their performance has been observed [6,7]. However, this performance was reached decreasing drastically the conversion efficiency of the transition radiation in a single layer of such a MWPC-based TRD. In order to circumvent this aspect, we designed and built several versions of a new prototype of TRD based on a double-sided pad readout electrode. The main idea is to increase the conversion efficiency, conserving the performance and the number of

\*Corresponding author. Tel.: +40 21 4042392; fax: +40 21 4574432.

E-mail address: [mpetro@ifin.nipne.ro](mailto:mpetro@ifin.nipne.ro) (M. Petrovici).

readout channels of the prototypes mentioned above. This can be reached by symmetrizing the counter structure relative to the readout electrode using a double-sided pad-plane electrode. The results of measurements with such a prototype are presented in this paper. The next section describes the construction scheme of the detector and the experimental setups used in tests with a  $^{55}\text{Fe}$  source and mixed secondary beams at the SIS accelerator of GSI, Darmstadt.  $^{55}\text{Fe}$  source and in-beam test results in terms of energy resolution, deposited energy distribution for  $e$  and  $\pi$  and position resolution are presented in Section 3. Section 4 describes the results in terms of the  $e/\pi$  rejection factor. The dependence of the most probable value of the pulse height and charge distributions as a function of counting rate is presented in Section 5. Section 6 is dedicated to the conclusions.

## 2. Description of the detectors and the test setup

### 2.1. Principal configuration and details of the prototype

A conceptual drawing of the prototype is shown in Fig. 1. The central readout electrode, dashed line in Fig. 1, separates the detector into two identical sections. It has a

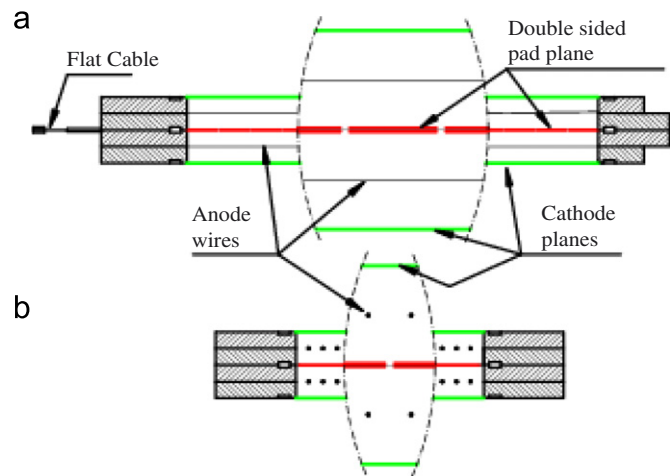


Fig. 1. Cross-sections through the detector: (a) parallel and (b) perpendicular to the direction of the wires.

pad structure on both sides, the corresponding pads on the upper and lower surface are connected. The two anodes, up and down relative to the central electrode, were made from gold plated tungsten wires of  $20\ \mu\text{m}$  diameter. The anode–cathode gap is 3 mm and the anode wire pitch is 2.5 mm, respectively. Aluminized mylar ( $25\ \mu\text{m}$ ) was used to close the gas volume providing at the same time the cathode of the respective MWPC. The photos in Fig. 2 show the inside of the detector before closing it with the gas windows or outer cathodes and the central double-sided electrode. Fig. 2 also shows the gas in- and outlets for each of the detector halves. The pad size is  $5 \times 10\ \text{mm}^2$ . Three versions of such a detector were built. One chamber was built with the central readout electrode made from a PCB of  $250\ \mu\text{m}$  thickness to test the basic functionality of the design. The readout electrode had two rows of nine pads on either side.

A second detector contained a  $3\ \mu\text{m}$  aluminized mylar foil ( $1.8\ \mu\text{g}/\text{cm}^2$  aluminium layer) without a pad structure as central readout electrode.

For the third variant of the detector the above-mentioned double-sided copper pad readout structure was etched on  $25\ \mu\text{m}$  kapton foil with the copper evaporated on it (see Fig. 2b).

### 2.2. Experimental setup

The detectors were tested using a  $^{55}\text{Fe}$  source. Custom built charge-sensitive preamplifier/shapers (gain:  $2\ \text{mV}/\text{fC}$ ; noise: 1800 electrons rms) were used to process the detector signals which were digitized by an AD811 peak sensing ADC. The MBS GSI-type data acquisition system has been used [8]. The source was carefully collimated onto the central pad to prevent the influence of electric field distortions at the edge of the chamber.

The in-beam tests were performed in a joint measurement campaign of the JRA4-I3HP Collaboration using the standard setup for ALICE–TRD tests [5], presented in Fig. 3. The components used in the analysis of these tests are: two silicon strip detectors for beam profile definition, two arrays of plastic scintillators for time-of-flight information, a Pb-glass calorimeter and a gas-filled Cherenkov detector for discriminating between  $e$  and  $\pi$ . The signals delivered by all pads were processed using a new generation

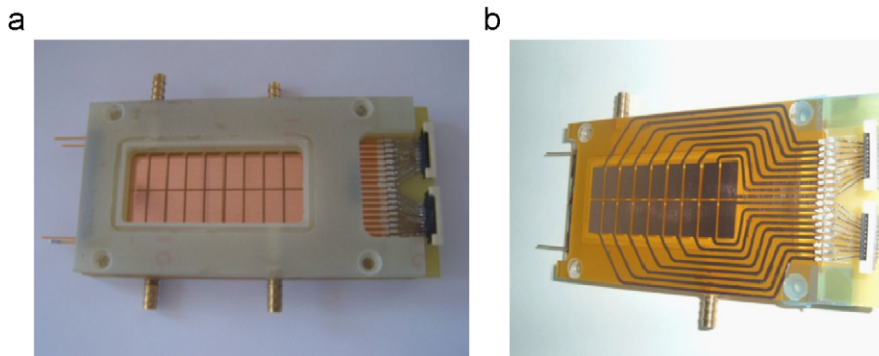


Fig. 2. A photograph of (a) the chamber structure before mounting the gas foils and (b) of the central electrode used for the third version (see the text).

of PASA front-end electronics [9]. They were digitized by an 8-bit non-linear Flash ADC (FADC) system with 25 MHz sampling frequency (0.6 V swing and an adjustable baseline) in conjunction with the above-mentioned acquisition system. Mixture of Ar/CO<sub>2</sub>(70%/30%) and Xe/CO<sub>2</sub>(85%/15%) were circulated through the counters during the source and in-beam tests.

### 3. Experimental results

#### 3.1. Source measurements

Typical amplitude (energy) spectra obtained in <sup>55</sup>Fe source tests are shown in Fig. 4 (anode wires (Fig. 4a) and pads (Fig. 4b)) for the first version of the prototype. The

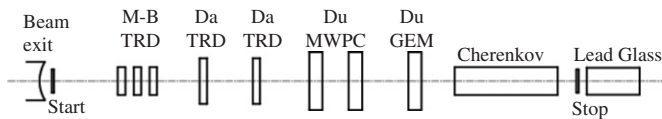


Fig. 3. Setup of the test beamline. Results from the three TRDs labeled M-B TRD (two version 3 types and one version 1 type) are discussed in this paper (other variants (Da TRD, Du MWPC, Du GEM) are not discussed here). Start and stop were generated from scintillator arrays of 4 NE102 strips. A gas Cherenkov counter and a lead glass calorimeter are used for particle identification.

worse energy resolution of 15.4% ( $\sigma$ ) using the pad information relative to 8.5% ( $\sigma$ ) corresponding to the anode signal is mainly due to the fact that only one row of pads was readout. Consequently, part of the signal shared between the two pad rows was missed.

Amplitude spectra for the second prototype are depicted in Fig. 4c. The energy resolution of 12.5% is mainly due to larger capacitance of the intermediate electrode compared to the wires. The pad size is equal with the active counter surface  $\sim 22 \times 50 \text{ mm}^2$ . For such an intermediate electrode absorption of X-rays is negligible, the measured value is 1.5% at 5.9 keV.

Fig. 4d presents the results obtained with prototype version 3. The resolution is comparable to the one obtained for the first version. The measured absorption in the intermediate electrode is 15%.

While the energy resolution is identical to the one-sided version, the conversion probability for 5.9 keV X-rays is increased owing to the second amplification volume in the double-sided version. The influence on the  $e/\pi$  discrimination performance will be demonstrated in Section 4.

#### 3.2. In-beam tests

The detectors discussed in this paper are labeled M-B TRD in the sketch of the experimental setup presented in Fig. 3.

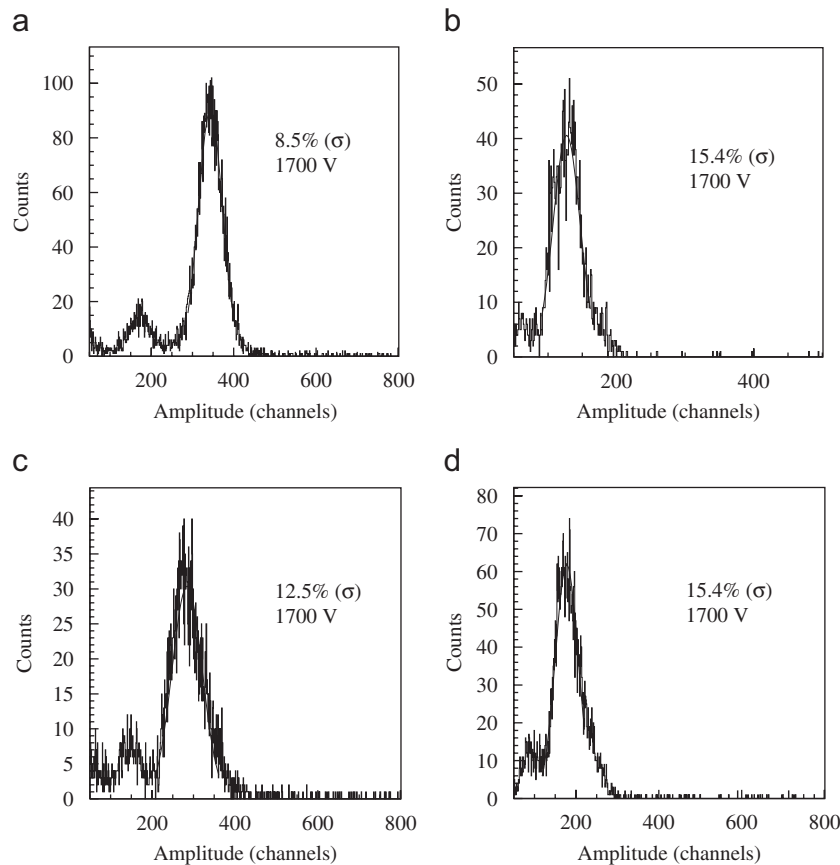


Fig. 4. The energy spectra of a <sup>55</sup>Fe source taking the signal from (a) version 1, anode electrode, (b) version 1, pad plane, (c) version 2, pad plane and (d) version 3, pad plane.

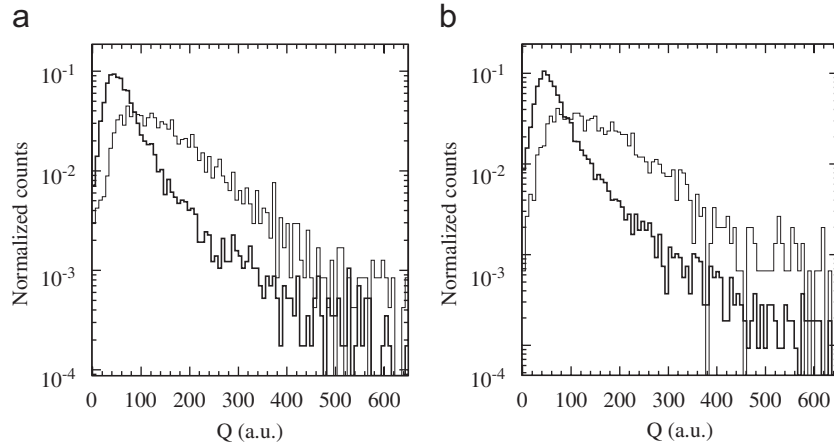


Fig. 5. Charge ( $Q$ ) distributions of electrons (thin line) and pions (thick line) for (a) 1.0 GeV/c and (b) 1.5 GeV/c using a Xe/CO<sub>2</sub>(85%/15%) gas mixture and an anode voltage of 1800 V. For both measurements a Rohacell radiator was used.

The prototypes were tested with different gas mixtures, gas gains, momenta and beam intensities. For all runs a structure of fibers of 17  $\mu\text{m}$  diameter of about 4.0 cm thickness and Rohacell HF71 of 2.0 cm thickness [5] was used as radiator. For the rest of the paper this combination will be called Rohacell.

In order to evaluate the performance of this radiator, a regular periodic polypropylene foil stack (120 foils, 20  $\mu\text{m}$  thickness, 500  $\mu\text{m}$  gap) was placed in front of one chamber for one run.

The charge ( $Q$ ) distribution of electrons and pions for 1.0 and 1.5 GeV/c momentum, respectively, a gas mixture of Xe/CO<sub>2</sub>(85%/15%) and an anode voltage of 1800 V are presented in Fig. 5. The double-sided configuration yields twice the signal for electrons and pions due to ionization energy loss. For electrons the signal owing to transition radiation (TR) is influenced by the increased conversion probability as well as by the absorption in the central electrode ( $\sim 15\%$ ).

The overall effect is that the peak of the deposited energy distribution due to direct ionization, specific for thin detectors, disappears, moving to larger values (of PH or  $Q$ ) due to the extra contribution of TRs converted with higher probability in a thicker detector. These conclusions are supported by the deposited energy distribution obtained with the single-sided prototype, based on a simple MWPC, presented in Fig. 6 [7].

The obtained position resolution for the third version of double-sided TRD prototype is better than 200  $\mu\text{m}$  for particle rates up to  $2 \times 10^5$  particles  $\text{cm}^{-2} \text{s}^{-1}$ . Details will be reported in a forthcoming paper [12].

#### 4. Pion rejection performance

The charge distributions presented in Fig. 7 were fitted using a superposition of a Landau and a Gaussian distribution. The fits were used in simulations in order to estimate the pion rejection factor as a function of the number of layers of such TRD detectors.

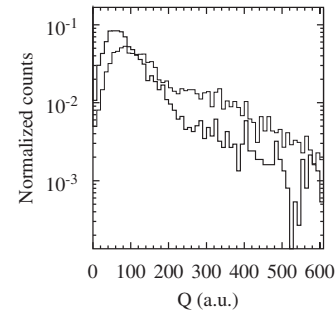


Fig. 6. Charge ( $Q$ ) distributions of electrons (thin line) and pions (thick line) for 1.0 GeV/c and a Xe/CO<sub>2</sub>(85%/15%) gas mixture for a single-sided high-counting-rate TRD at 1900 V anode voltage.

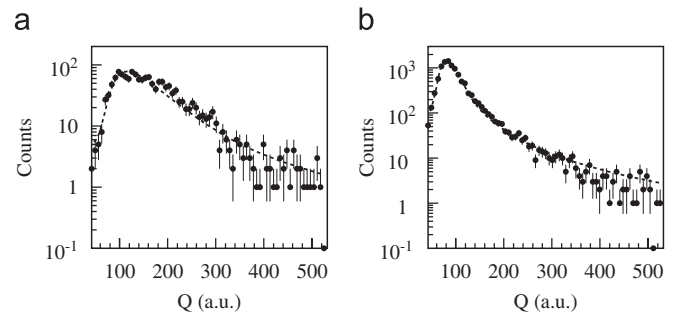


Fig. 7. Experimental charge distributions (points) for electrons (a) and pions (b) fitted with a superposition of Landau and Gauss functions (dashed lines), for a Xe/CO<sub>2</sub>(85%/15%) gas mixture and 1800 V applied voltage, used as input for the Monte Carlo simulation.

The pion rejection factor was extracted using the likelihood on integrated energy deposit [13]. For an energy deposit  $E_i$  in layer  $i$ ,  $P(E_i|e)$  is the probability to be produced by an electron and  $P(E_i|\pi)$  is the probability to be produced by a pion. The likelihood  $L$  to be an electron is

$$L = P_e / (P_e + P_\pi)$$

where

$$P_e = \prod_{i=1}^N P(E_i|e)$$

$$P_\pi = \prod_{i=1}^N P(E_i|\pi).$$

Here  $N$  denotes the number of simulated layers.

The pion efficiency at 90% electron efficiency for 1.5 GeV/c momentum as a function of the number of

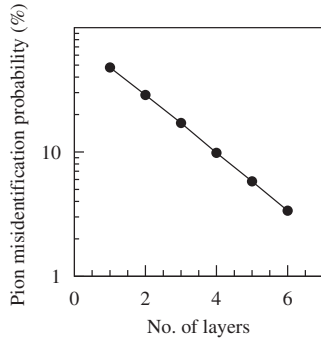


Fig. 8. Pion efficiency at 90% electron efficiency at 1.5 GeV/c momentum as a function of the number of layers for the Rohacell radiator and an anode voltage of 1800 V.

layers for the Rohacell radiator and an anode voltage of 1800 V is shown in Fig. 8. For a six layer configuration a pion efficiency of 3.3% is reached. A direct comparison of the results obtained with the Rohacell radiator and the polypropylene foil stack is presented in Fig. 9 for an anode voltage of 1700 V.

For such a regularly spaced radiator an efficiency of 1.1% is obtained for a six layer structure. At the same voltage, a pion efficiency of 5.4% for a six layer configuration is reached for Rohacell radiator. The performance of the regular foil stack is almost a factor of 5 better for the six layer configuration.

If we apply this correction factor to the previous run (at 1800 V anode voltage), the final estimated pion efficiency for six layer configuration and a 20/500/120 stack foil radiator is 0.7%.

### 5. Rate performance

In the previous sections the performance of the new prototype of TRD in terms of energy resolution, position resolution and pion efficiency was presented. Another important aspect of the anticipated experiments is the rate stability of the detectors. The effect of the high-counting-rate environment on the detector performance was tested using a mixture of positive particles of 1.5 GeV/c momentum in which protons were the dominant component. The counting rate per detector area was changed by varying the extraction time of the beam at a given beam intensity. Using the time-of-flight spectrum, protons were selected for the pulse height analysis and charge analysis.

The most probable values for the pulse height and charge were extracted from Landau fits. They are plotted as a function of counting rate in Fig. 10. Up to a counting rate of more than  $\sim 200 \times 10^3$  particles  $\text{cm}^{-2} \text{s}^{-1}$  virtually no deterioration of these values is observed.

As far as the pion efficiency as a function of counting rate is concerned, in Fig. 11a and b the pulse height distributions of hadrons and electrons, at different counting rates ( $26 \times 10^3$ ,  $110 \times 10^3$ , and  $250 \times 10^3$  particles  $\text{cm}^{-2} \text{s}^{-1}$ ), are presented. Within experimental errors no discernable deterioration is observed. We conclude that

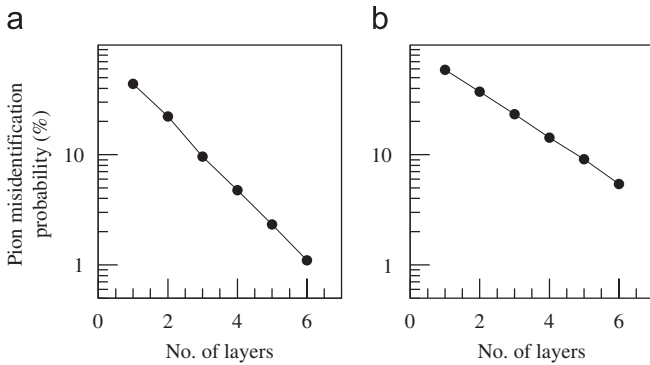


Fig. 9. Pion efficiency at 90% electron efficiency at 1.5 GeV/c momentum as a function of the number of layers for an anode voltage of 1700 V: (a) a stack of polypropylene foils with a regular periodic structure 20/500/120; (b) Rohacell radiator.

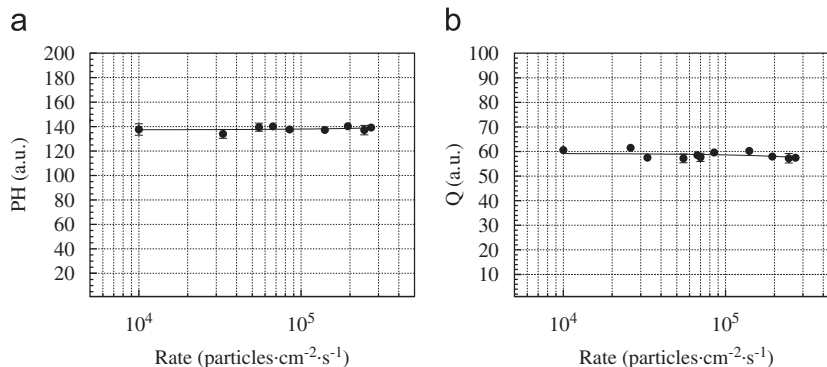


Fig. 10. The most probable values of the Landau fit of the pulse height and charge distributions as a function of counting rate.

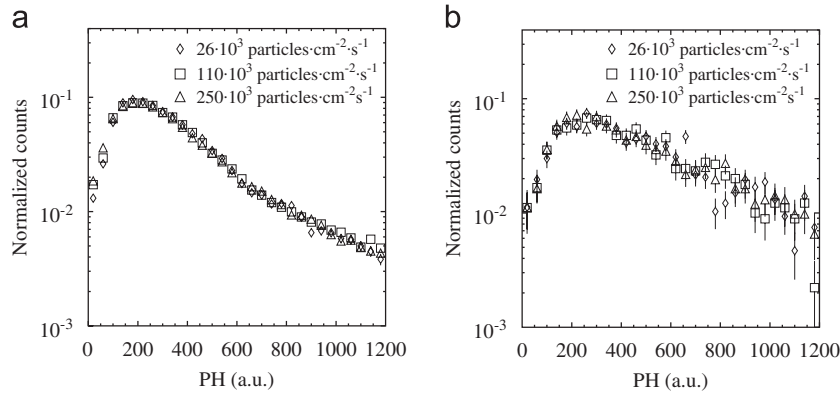


Fig. 11. Pulse height distributions of: (a) hadrons and (b) electrons for  $26 \times 10^3$ ,  $110 \times 10^3$ , and  $250 \times 10^3$  particles  $\text{cm}^{-2} \text{s}^{-1}$  counting rates.

these detectors preserve their pion efficiency performance up to more than  $200 \times 10^3$  particles  $\text{cm}^{-2} \text{s}^{-1}$ .

## 6. Summary and outlook

For electron–pion discrimination in high-counting-rate environment a new prototype of TRD based on a double-sided pad readout electrode was designed, built and tested. First results of measurements using a  $^{55}\text{Fe}$  source and mixed beams of electrons and pions have been presented in this paper.

The performance of this new type of TRD in terms of counting rate and pion efficiency recommends this principle of TRD as a solution for high-counting-rate environment and high-pion efficiency TRDs with reduced number of channels and material budget at a given granularity.

## Acknowledgments

This work was supported by JRA4-I3HP Contract no. 506078. The project receives support through EU-FP6 and CORINT-EU no. 58 financed by the Romanian National

Authority for Scientific Research. We would like to thank all participants of the JRA4 involved in TRD R&D activities. Special thanks to the SIS crew for the beam quality.

## References

- [1] CBM, Technical Status Report, 2005.
- [2] FAIR Baseline Technical Report, (<http://www.gsi.de/fair/report/btr.html>).
- [3] T. Akesson, et al., Nucl. Instr. and Meth. A 449 (2000) 464; T. Akesson, et al., Nucl. Instr. and Meth. A 522 (2004) 131.
- [4] ATLAS Collaboration, Inner Detector Technical Design Report, vols. I & II, CERN/LHCC/97-17 (1997)/hep-ex/0311058.
- [5] ALICE-Collaboration, J. Phys. G 30 (2004) 1517.
- [6] A. Andronic, et al., GSI Science Report 2005-1, INSTMETH-33.
- [7] M. Petris, et al., Nucl. Instr. and Meth. A, submitted for publication.
- [8] H.G. Essel, N. Kurz, GSI Annual Report, 1998, p. 188.
- [9] H.K. Soltveit, J. Stachel, GSI Science Report 2005-1, INSTMETH-34.
- [12] M. Klein-Bösing, et al., Nucl. Instr. Meth. (2007), submitted for publication.
- [13] A. Büngener, et al., Nucl. Instr. and Meth. 214 (1983) 261.